Supporting Information

X-ray Spectroscopy Characterization of Cobalt Stabilization within a Monolayer Carbon Nitride in Oxygen Evolution Reaction

Anders K. Vestergaard[a],[†] Jens Jakob Gammelgaard[a],[†] Zhaozong Sun,[†] Siqi Zhao,[‡,¶] Zheshen Li,[§] Nina Lock,[‡,¶,‖] Kim Daasbjerg,[†,¶,‡] and Jeppe V. Lauritsen[*,†]

†*Interdisciplinary Nanoscience Center (iNANO), Aarhus University, 8000 Aarhus C, Denmark*

‡*Novo Nordisk Foundation (NNF) CO_2 Research Center, Aarhus University, 8000 Aarhus C, Denmark*

¶*Department of Chemistry, Aarhus University, 8000 Aarhus C, Denmark*

§*Department of Physics and Astronomy, Aarhus University, 8000 Aarhus C, Denmark*

‖*Department of Biological and Chemical Engineering, Aarhus University, 8200 Aarhus N, Denmark*

E-mail: jvang@inano.au.dk

[a]Authors contributed equally

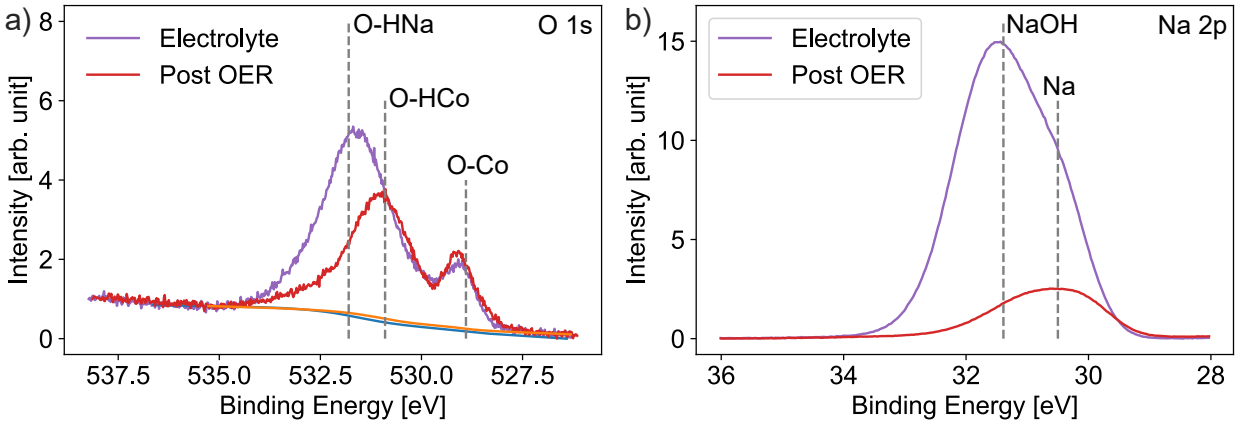

Figure S1: O 1s and Na 2p spectra. **(a)** The O 1s spectra can be described with a 3-peak model. A CoO peak at low energies (528.9 eV), a CoOOH peak (530.9 eV), and a NaOH peak (531.8 eV). The binding energies for CoO and CoOOH closely match literature.[1] The three peaks match the expectation from the Co 2p spectra well, as we find both the cobalt oxide and hydroxide in the O 1s as well as the Co 2p spectra. **(b)** Na 2p spectra, where the intensities are normalized by scan number and slit, such that they are representative of relative Na concentrations on the surface. The clear NaOH peak (31.39 eV) observed in the O 1s spectrum of the electrolyte-dipped sample is also present in the Na 2p spectrum. There is also a Na(0) signal (30.5 eV). Both energies match literature values.[2] Both of these signals are also present for the Post OER sample, but the Na(0) signal is the dominant one. However, both the amount and oxidation state of Na seems to be highly influenced by the drying process when the sample is returned to vacuum.

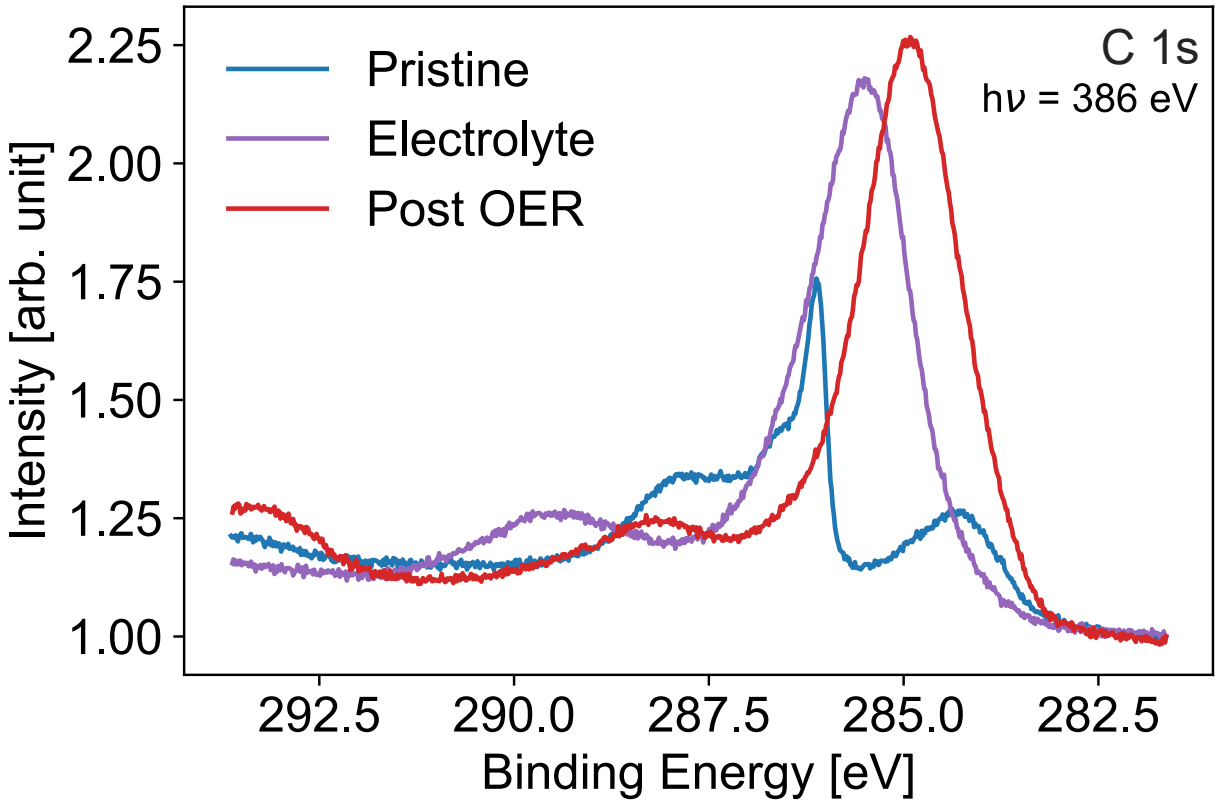

Figure S2: C 1s spectra of the three samples: pristine CoCN on Au(111) (blue), CoCN dipped in electrolyte (purple) and CoCN post OER (red). The two samples that have been exposed to the electrochemical cell and electrolyte are dominated by adC.

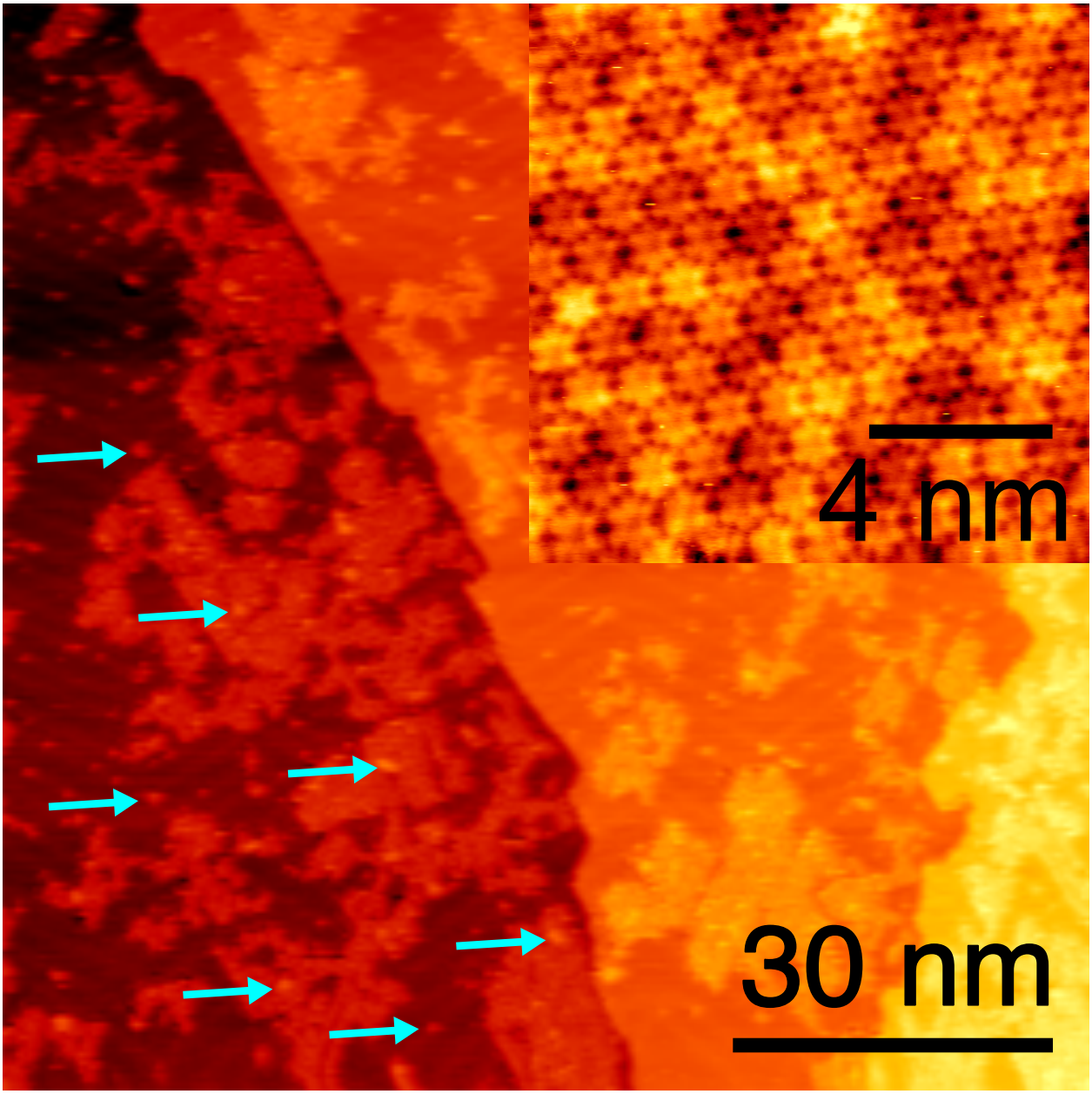

Figure S3: STM image of the as-prepared CoCN sample prior to measuring 100 rounds of cyclic voltammetry. Arrows indicate positions of some of the Co NPs. Inset in top right corner shows high resolved pristine CoCN. Scanning parameters for large scale image: I_t = 0.35 nA and V_t = 878.9 mV. Inset: I_t = 0.39 nA and V_t = 50.4 mV.

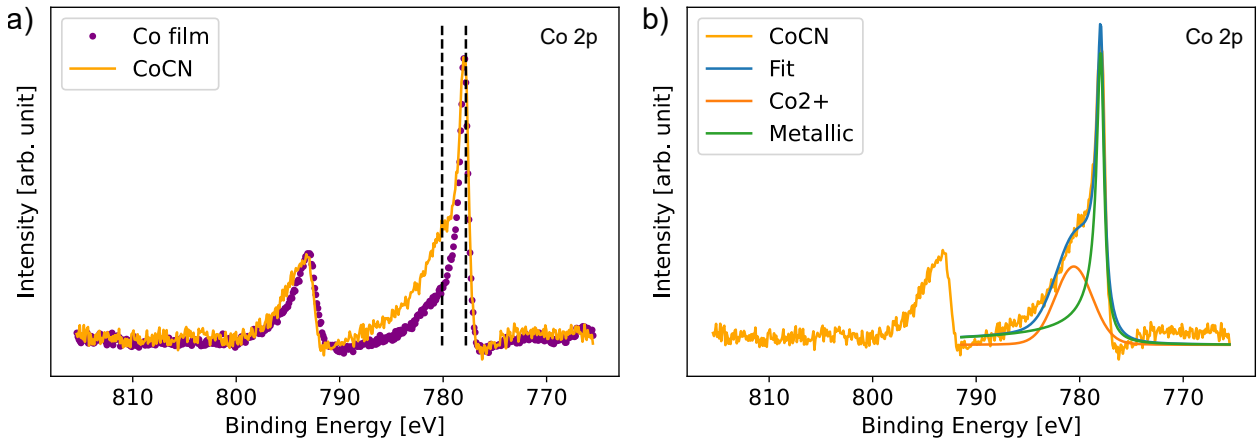

Figure S4: XPS Co 2p spectra of CoCN. a) Comparison of Co2p spectra from CoCN and metallic Co film. Dashed black lines indicate energy of Co^0 and Co^{2+}. CoCN has a clear shoulder from Co^{2+} from Co coordinated in the CoCN monolayer. The metallic contribution is from Co nanoparticles. b) Fit of Co $2p_{3/2}$ with two components: one from Co^{2+} and one from metallic Co. The Co^{2+} and metallic Co contribute with 34 % and 66 % of the intensity, respectively.

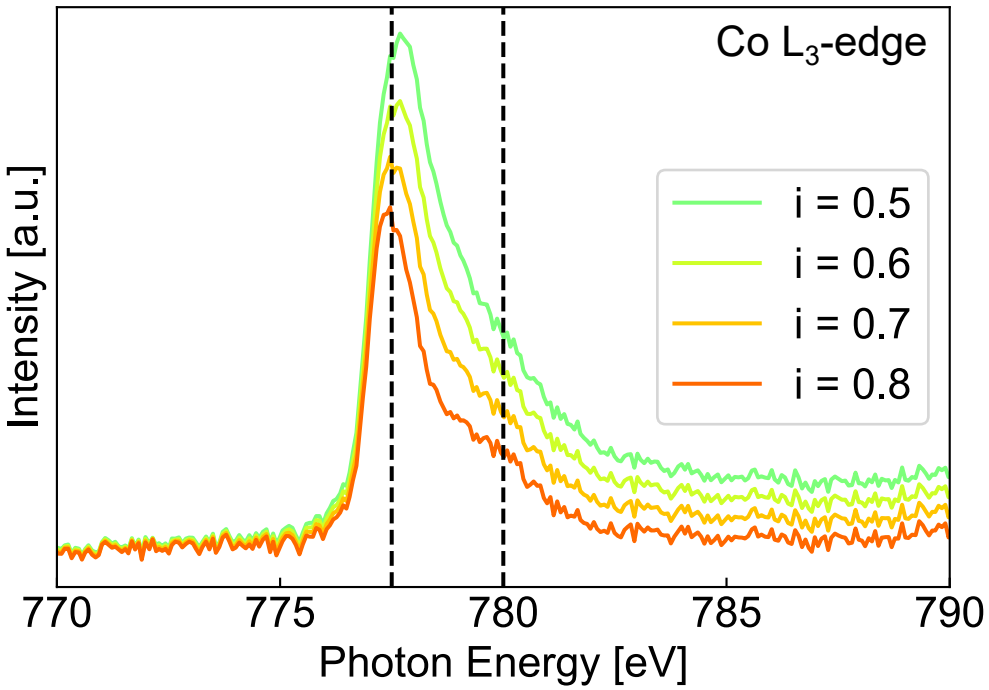

Figure S5: Co L_3-edge of CoCN subtracted by varying amounts of contribution from Co NPs. This is achieved by subtracting the background corrected Co NP spectrum from the background corrected CoCN spectrum, with i denoting the relative amount of Co NP in CoCN. The results show the multiplet structure of the CoCN to be less pronounced than what would be expected when comparing to bulk references of materials with Co(II) in square planar geometry. However, for monolayer structures the substrate interacts with the adsorbed species (here Co) resulting in a charge-transfer that can alter the adsorption profile by quenching some of the states present in bulk samples.[3,4] We speculate that this coupling and charge-transfer ties back to the coupling mentioned between C/N and the continuum of states in the Au(111) conduction band, and potentially Co is the origin for the coupling to the substrate.

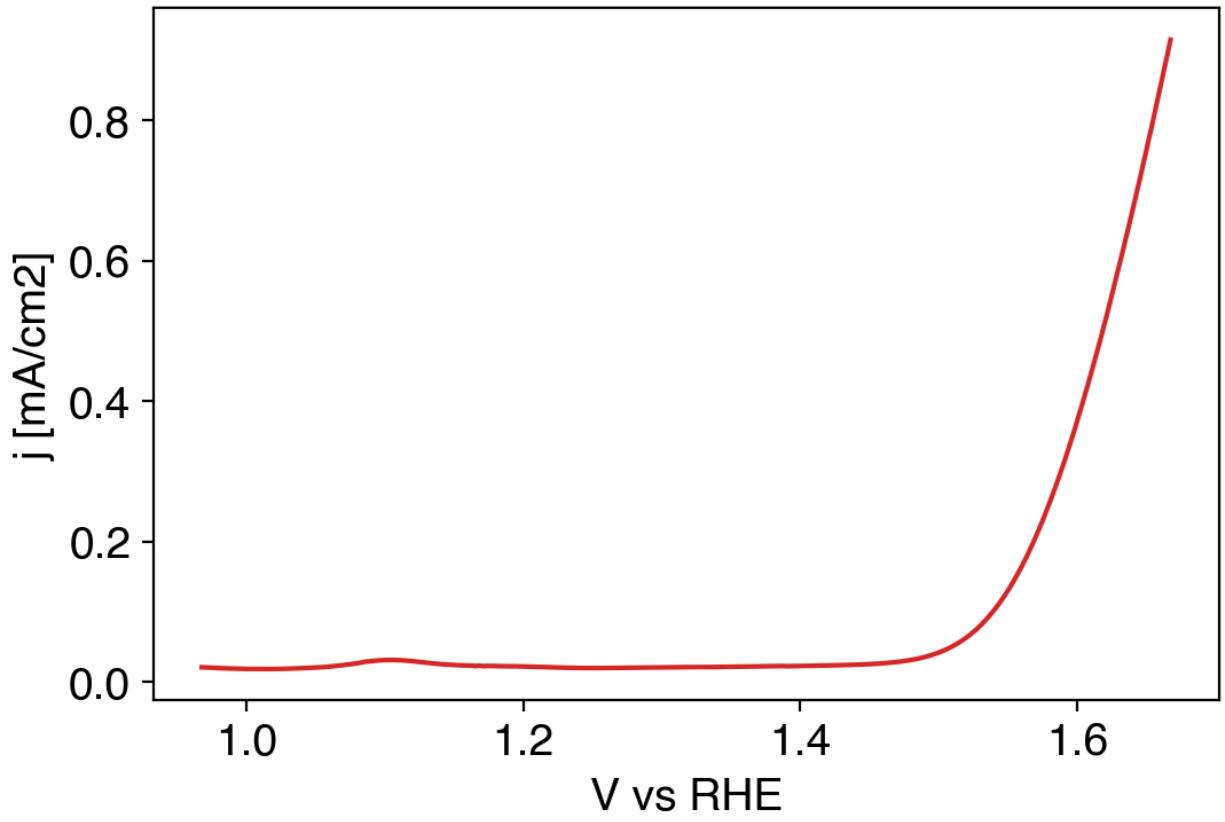

Figure S6: Linear sweep measurement of the CoCN, leading to the sample termed "Post OER" in Figure 4 and Figure 5.

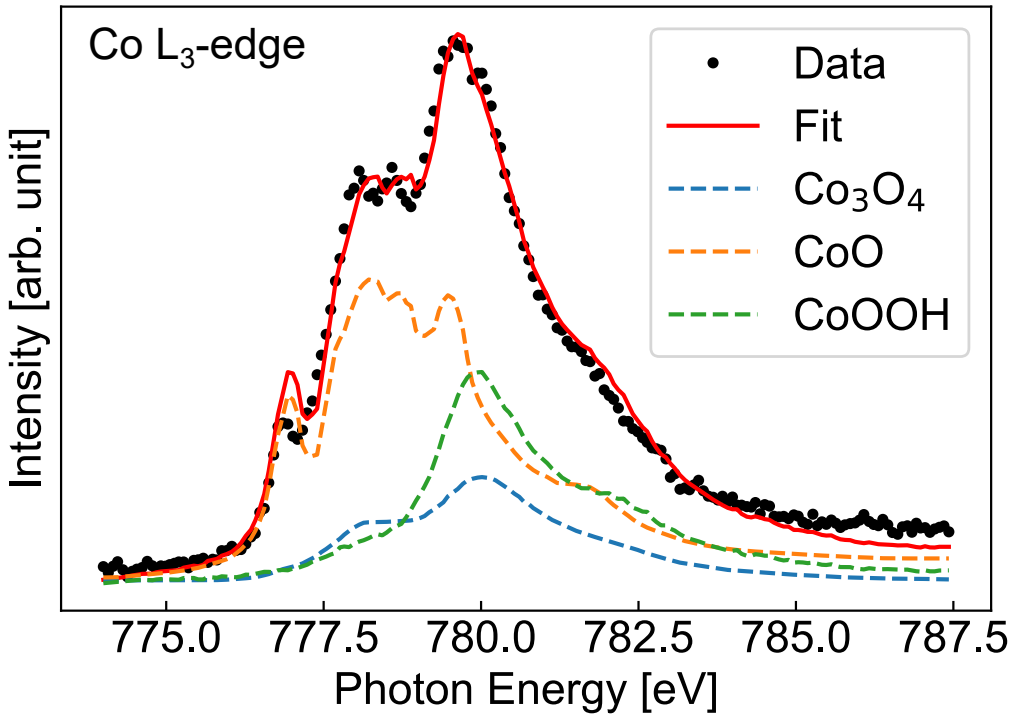

Figure S7: Linear combination fit Co L_3-edge of CoCN/Au post OER. Based on the fit, the CoCN/Au consists of 46% CoO, 27% CoOOH, and 26% Co_3O_4. The three peaks at 776.8-778.6 eV mainly originates from CoO, while the peak at 779.6 eV is primarily from a combination of CoOOH and Co_3O_4. The reference spectra of CoO and Co_3O_4 are adapted from Galakhov[5] and reference spectrum of CoOOH is adapted from Kudielka.[6]

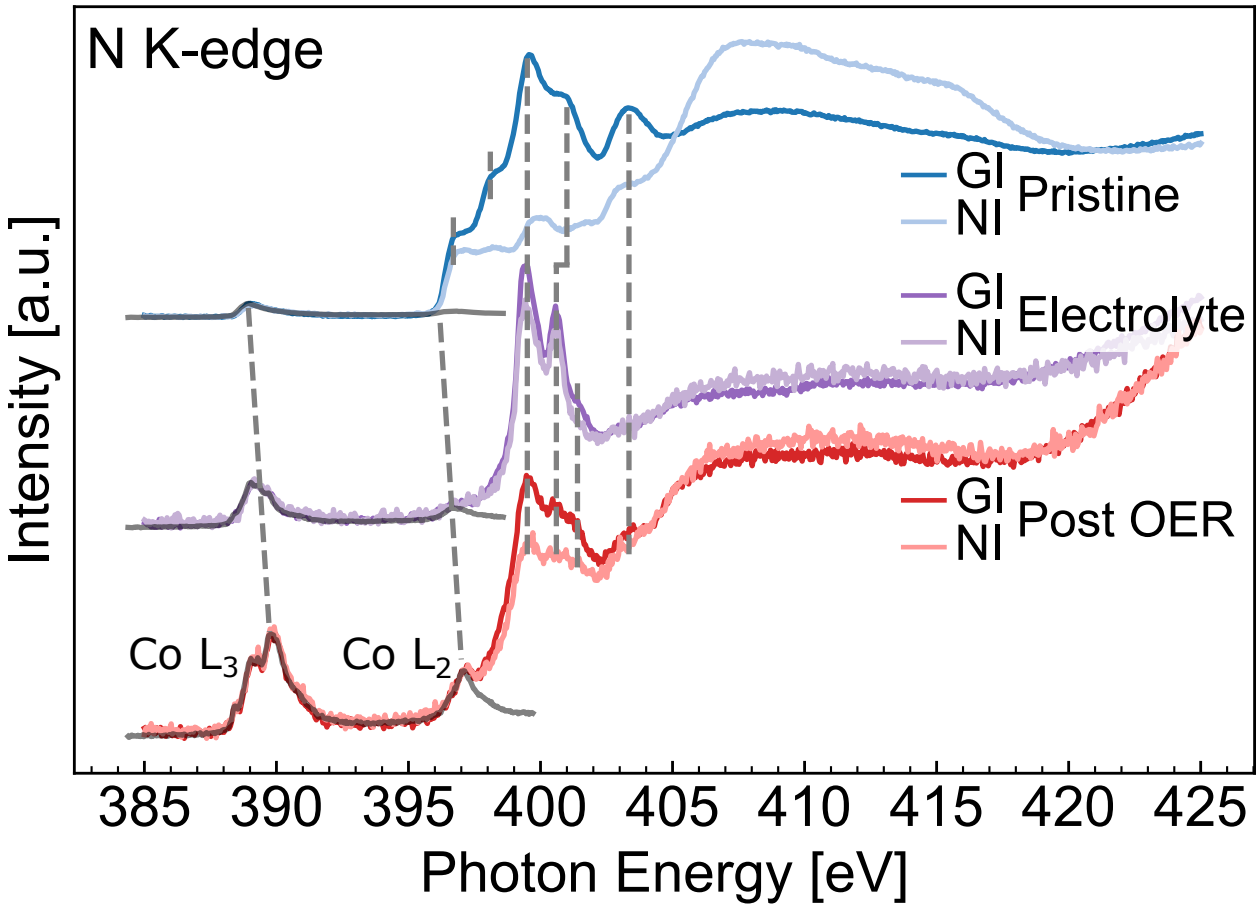

Figure S8: NEXAFS N K-edge spectra of CoCN/Au. At 385-400 eV a grey line is fitted to the N K-edge spectra based on the Co L-edge spectra from the respective samples. The origin of the peaks is from 2nd order light produced by the beamline optics. Light with double energy (half wavelength) will unavoidably also be produced. This light results in excitations of both the Co L_3 and Co L_2 edges.

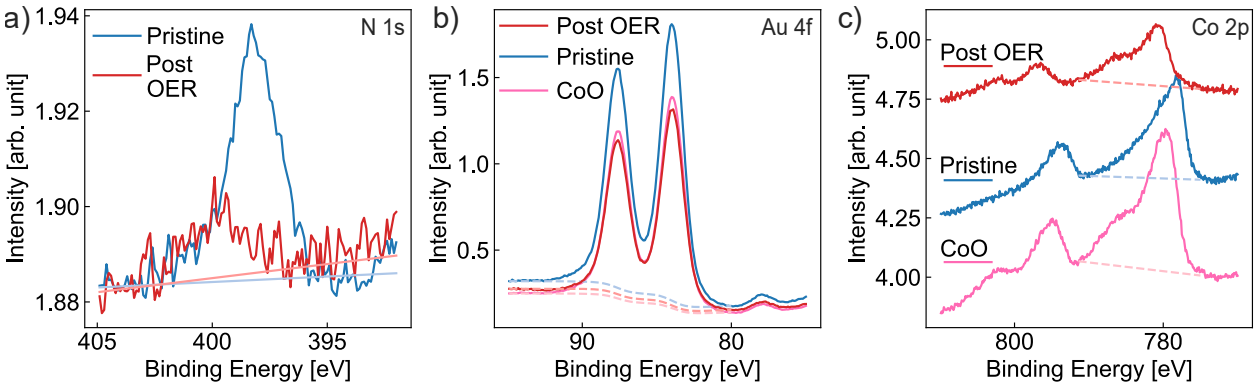

Figure S9: Quantitative XPS results for the CoCN measured over 100 CV cycles. The pristine CoCN is 0.6 ML, while the CoO is 0.3 ML. **(a)** N 1s spectra and backgrounds for the pristine sample and the sample after 100 cycles, the intensity of the oxidized sample is 28% of the initial intensity. **(b)** Au 4f spectra for CoO, pristine CoCN, and the oxidized sample. The Au signal of the oxidized sample is attenuated to 69% of the pristine sample. **(c)** Co 2p spectra and background for CoO, pristine CoCN, and the oxidized sample. The oxidized sample has 42% of the intensity of the pristine sample, implying a loss of cobalt of approximately 40%, after accounting for the general attenuation due to adsorbents. The oxidized sample has 46% of the Co as the CoO sample after accounting for the relative Au 4f intensities.

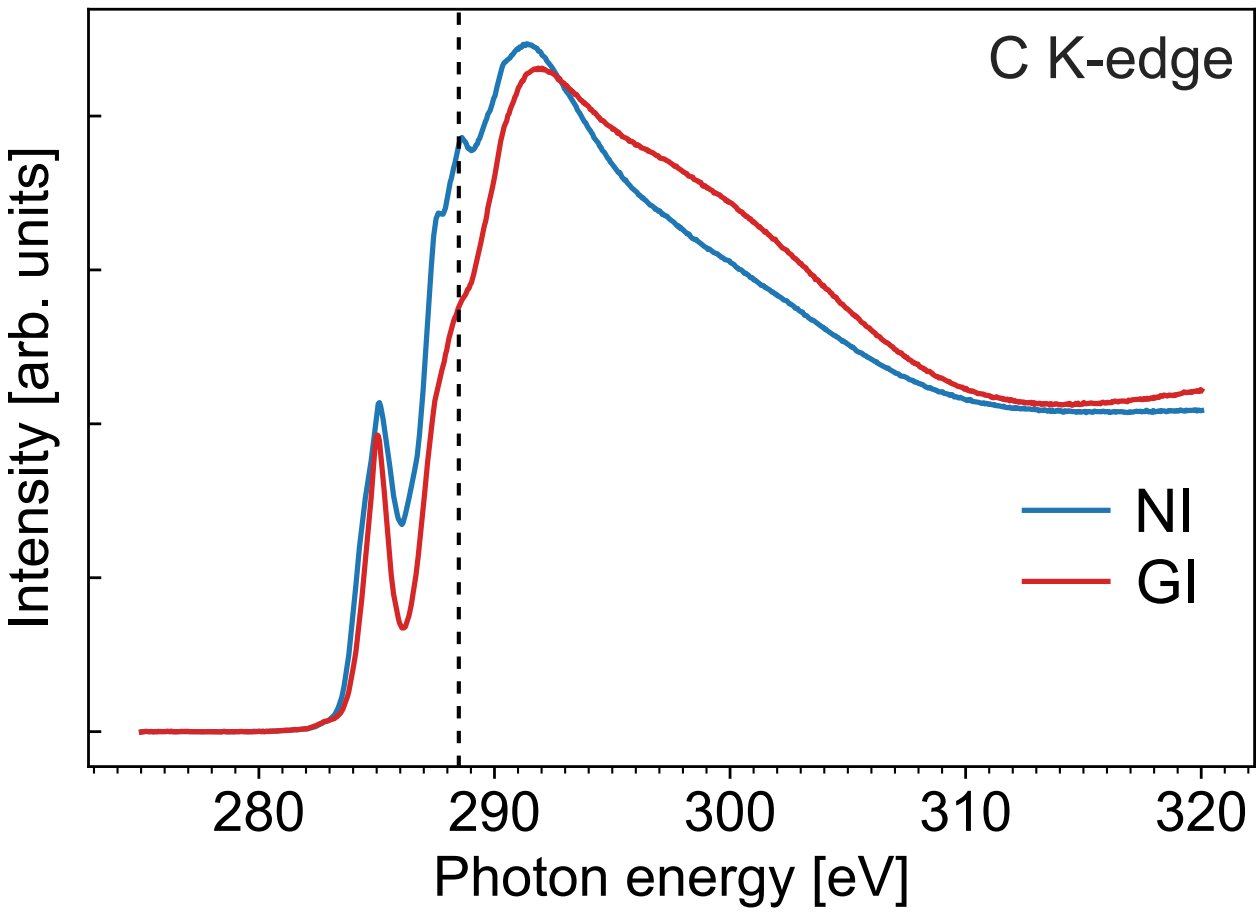

Figure S10: C K-edge spectrum from clean Au(111) sample after exposure to electrolyte and sweeping to ORR potentials. The carbon present on the sample is adC from contact with the electrolyte and from transfer back to the UHV environment from the EC cell. Dashed line indicate the position of the C_{3N} of the CoCN.

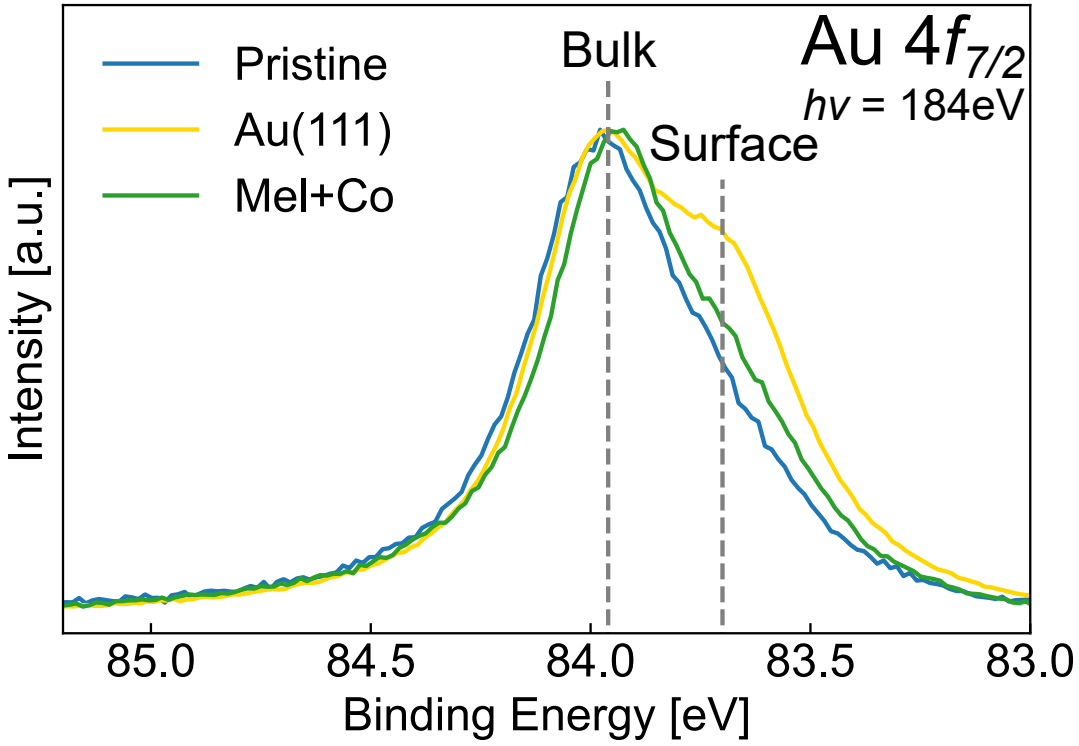

Figure S11: Au $4f_{7/2}$ XP spectra for three different samples. The clean Au(111) (yellow), the pristine CoCN (blue) and unreacted melamine mixed with Co (green). The pristine CoCN suppresses the surface component of Au(111) more effectively than adding melamine and Co separately. Furthermore, the pristine sample is only 0.6 ML, while the melamine coverage is above 1 ML. During synthesis of CoCN excess melamine is evaporated from the surface due to the temperature, which limits the total coverage to follow the availability of Co atoms. Thus, it is clear the the weaker surface signal in the pristine CoCN compared to the mixed melamine and Co sample must be due to a strong interaction between CoCN and Au(111).

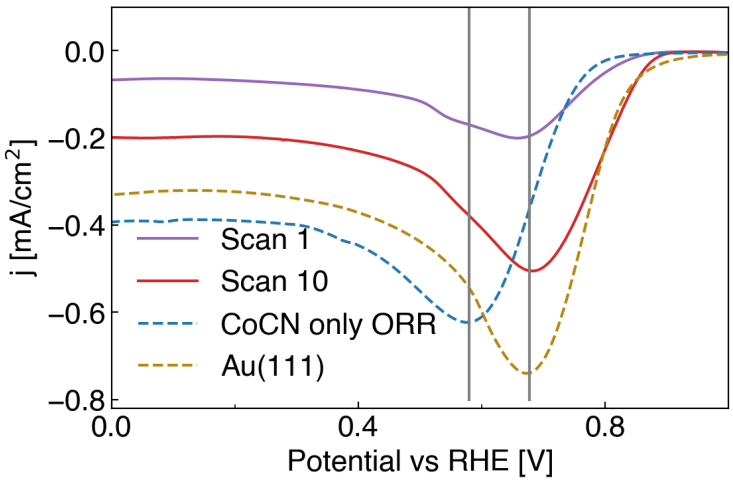

Figure S12: Electrochemical measurements on three different samples. Two scans from the CoCN/Au sample studied in Figure 1. A pristine 0.7 ML CoCN swept only in the reductive region (between -0.24 and 1.37 V_{RHE}) in O_2 saturated 0.1 M NaOH (blue dash), a clean Au(111) crystal swept between -0.24 and 1.37 V_{RHE} in O_2 saturated 0.1 M NaOH (gold dash). From the sample studied in Figure 1, scan 1 (purple line) and scan 10 (red line) show large differences. The CoCN (ORR only) and Au(111) samples show different peak and onset potentials. Two vertical grey lines have been added at the peak potentials to guide the eye. Looking at scan 1 for CoCN/Au, it is clear that there are two peaks, one at the CoCN potential and one at the Au(111) potential. At scan 10 the Au(111) peak is much more significant, while a slight bump is still visible at the CoCN potential. The increase in current is assigned to increased oxygen presence at the surface, which is produced during OER. All measurements are made in 0.1 M NaOH at 50 mV/s.

The increased ORR activity shown in Figure 1b can also be readily explained under this model. The CoCN sample is active towards ORR,[7] and the initial activity reflects this intrinsic activity. As the structure is transformed during the oxidative sweep, the activity of CoCN is likely lost. However, the observed activity increases. This activity is the result of changing from CoCN as the active catalyst to Au(111). Au(111) is an active ORR catalyst, where the step edges are the active sites.[8] The CoCN grows preferentially at the kinks of the herringbone and at step edges.[7] Therefore, at the outset of electrochemical measurements, the almost atomically flat Au(111) surface is inactivated by the CoCN, through the Au steps being covered by CoCN. However, as the surface grows progressively rougher during each OER cycle, the number of uncovered steps increases, which in turn leads to increased activity. This development is evident in On the first scan of the CoCN/Au system, it is first swept to oxidative potentials, and upon reaching reductive potentials the ORR sets in, here the ORR peak has two components, one at the potential characteristic of CoCN and one at the potential characteristic of Au(111). After 10 sweeps only the Au(111) component is observed. The lack of a strong ORR signal for the pure Au(111) crystal in Figure 1a is explained by lower oxygen concentration at the surface. For the CoCN/Au the majority of the increase in current is a result of increasing oxygen concentration in the electrolyte as a result of the OER being performed.

References

(1) Holt, A. J. U.; Pakdel, S.; Rodríguez-Fernández, J.; Zhang, Y.; Curcio, D.; Sun, Z.; Lacovig, P.; Yao, Y.-X.; Lauritsen, J. V.; Lizzit, S.; Lanatà, N.; Hofmann, P.; Bianchi, M.; Sanders, C. E. Electronic properties of single-layer CoO_2/Au(111). *2D Mater.* **2021**, *8*, 035050.

(2) Citrin, P. H. High-Resolution X-Ray Photoemission from Sodium Metal and Its Hydroxide. *Phys. Rev. B* **1973**, *8*, 5545–5556.

(3) Glaser, M.; Peisert, H.; Adler, H.; Aygül, U.; Ivanovic, M.; Nagel, P.; Merz, M.; Schuppler, S.; Chassé, T. Electronic Structure at Transition Metal Phthalocyanine-Transition Metal Oxide Interfaces: Cobalt Phthalocyanine on Epitaxial MnO Films. *J. Chem. Phys.* **2015**, *142*, 101918.

(4) Stepanow, S.; Miedema, P. S.; Mugarza, A.; Ceballos, G.; Moras, P.; Cezar, J. C.; Carbone, C.; de Groot, F. M. F.; Gambardella, P. Mixed-Valence Behavior and Strong Correlation Effects of Metal Phthalocyanines Adsorbed on Metals. *Phys. Rev. B* **2011**, *83*, 220401.

(5) Galakhov, V. R. X-Ray Spectroscopy of Cobaltites. *Physics of Metals and Metallography* **2021**, *122*, 83–114.

(6) Kudielka, A.; Schmid, M.; Klein, B. P.; Pietzonka, C.; Gottfried, J. M.; Harbrecht, B. Nanocrystalline cobalt hydroxide oxide: Synthesis and characterization with SQUID, XPS, and NEXAFS. *Journal of Alloys and Compounds* **2020**, *824*, 153925.

(7) Gammelgaard, J. J.; Sun, Z.; Vestergaard, A. K.; Zhao, S.; Li, Z.; Lock, N.; Daasbjerg, K.; Bagger, A.; Rossmeisl, J.; Lauritsen, J. V. A Monolayer Carbon Nitride on Au(111) with a High Density of Single Co Sites. *ACS Nano* **2023**, *17*, 17489–17498.

(8) Štrbac, S.; Anastasijević, N.; Adžić, R. Oxygen reduction on Au(111) and vicinal Au(332) faces: A rotating disc and disc-ring study. *Electrochim. Acta* **1994**, *39*, 983–990.